

A witness for coherent electronic oscillations in ultrafast spectroscopy

Joel Yuen-Zhou, Jacob J. Krich, and Alán Aspuru-Guzik*

Department of Chemistry and Chemical Biology, Harvard University, Cambridge, MA 02138

We report a conceptually straightforward witness that isolates coherent electronic oscillations from their vibronic counterparts in nonlinear optical spectra of molecular aggregates: Coherent oscillations as a function of waiting time in broadband pump/broadband probe spectra correspond to coherent electronic oscillations. Oscillations in individual peaks of 2D electronic spectra do not necessarily yield this conclusion. Our witness is simpler to implement than quantum process tomography and potentially resolves a long-standing controversy on the character of oscillations in ultrafast spectra of photosynthetic light harvesting systems.

Recently, there has been considerable interest in long-lived quantum superpositions of electronic states in photosynthetic molecular aggregates and their potential role in efficient energy transport in biological conditions [1, 2]. Evidence for such electronic coherences stems from time oscillations in peaks of two-dimensional electronic spectra (2D-ES) which persist for over 600 fs [3–5]. However, coherences between vibronic levels involving a single electronic state exhibit similar signatures in 2D-ES [4, 7, 8] and have been shown to nontrivially affect energy transfer [9–11]. Although there are additional hints that support the interpretation of the oscillations as due to electronic states (beating frequencies and comparison with all-atom simulations [12]), unambiguous tools to experimentally unravel the nature of these oscillations are required. A big step has been the observation that, under weak coupling to vibrations and negligible coherence transfer processes, electronic coherences imply oscillations in off-diagonal peaks of rephasing 2D-ES and in diagonal peaks of their non-rephasing counterparts [13], whereas general vibronic coherences show up as oscillations in any region of either spectra [14]. However, the rephasing 2D-ES of the paradigmatic Fenna-Matthews-Olson (FMO) complex exhibits oscillations in both diagonal and off-diagonal peaks, indicating that systems of interest may lie in the regime of strong coupling to vibrations [15] or exhibit vibronic coherences only [8]. Techniques of wavepacket reconstruction [7] or quantum process tomography (QPT) [17, 18] should clearly provide an answer at a cost of several experiments. Our purpose here is to provide a practical witness for coherent electronic oscillations, which is applicable across different regimes of weak and strong coupling to vibrations.

We illustrate the witness by considering the simplest molecular exciton model, the coupled dimer [17]. Its Hamiltonian is given by $H_0(\mathbf{R}) = T_N + H_{el}(\mathbf{R})$, where T_N is the nuclear kinetic energy, and $H_{el}(\mathbf{R})$ is the electronic Hamiltonian which depends on the nuclei \mathbf{R} , $H_{el}(\mathbf{R}) = \sum_{mn} V_{mn}(\mathbf{R})|mn\rangle\langle mn| + J(\mathbf{R})(|10\rangle\langle 01| + |01\rangle\langle 10|)$. $|mn\rangle$ denotes the electronic state with m, n excitations in the first, second molecules, respectively ($m, n \in \{0, 1\}$), $V_{mn}(\mathbf{R})$ is the corresponding diabatic potential energy surface, and $J(\mathbf{R})$ is the coupling between site excita-

tions. Any pure state $|\Psi\rangle$ may be expressed in terms of vibronic states, that is, product states of the electronic (system) and nuclear (bath) degrees of freedom, $|\Psi\rangle = \sum_i a_i |e_i\rangle |N_i\rangle$, for coefficients a_i , and $\{|e_i\rangle, |N_i\rangle\}$ electronic and nuclear bases. A reduced electronic description of $|\Psi\rangle$ is obtained by performing a trace over the bath, $\rho_{el} = \text{Tr}_{nuc}(|\Psi\rangle\langle\Psi|)$. We consider light-matter perturbation in the dipole approximation, $H_{pert}(s) = -\boldsymbol{\mu} \cdot \boldsymbol{\epsilon}(\mathbf{r}, s)$, where $\boldsymbol{\mu} = \sum_{e=01,10} (\boldsymbol{\mu}_{eg}|e\rangle\langle g| + \boldsymbol{\mu}_{fe}|f\rangle\langle e|) + \text{h.c.}$ is the dipole operator, and $\boldsymbol{\epsilon}(\mathbf{r}, s) = \sum_{p=P,P'} [\epsilon_p(s - t_p)\mathbf{e}_p + \text{c.c.}]$ denotes the pump (P) and probe (P') pulses, with $\epsilon_p(s - t_p) = \frac{\lambda}{\sqrt{2\pi\sigma^2}} e^{-i\omega_p(s-t_p) - (s-t_p)^2/2\sigma^2}$ the Gaussian time-profile. Here, λ , ω_p , t_p , σ , and \mathbf{e}_p , are the strength, carrier frequency, center time, width, and polarization of the p -th pulse, respectively. We shall discuss PP' spectra $S_{PP'}(T)$ as a function of $T = t_{P'} - t_P$ (waiting time) [1], which can be recovered from a 2D-ES by integration along both frequency axes (Supplementary Material [21] sec. I, SI-I). The main result of this article is: *In the Condon approximation and the broadband limit ($\sigma \rightarrow 0$), oscillations of $S_{PP'}(T)$ as a function of T correspond to coherent electronic oscillations*; in this limit, $S_{PP'}(T)$ may be expressed solely in terms of reduced electronic states ρ_{el} , so oscillations cannot be due exclusively to nuclear dynamics.

The PP' signal may be written as the sum of $S_{SE}(T)$, $S_{ESA}(T)$, and $S_{GSB}(T)$, with separate contributions from stimulated emission (SE), excited state absorption (ESA), and ground state bleach (GSB) [3]. If the initial vibrational state is known, each of these terms may be expressed as a suitable wavefunction overlap (SI-I [21]). For example, let the initial wavefunction (before any pulse) be $|\Psi_0(0)\rangle = |g\rangle|\nu_i^{(g)}\rangle$, where $|\nu_i^{(\eta)}\rangle$ is a vibrational eigenstate of $H_{vib,\eta}(\mathbf{R}) \equiv T_N + V_\eta(\mathbf{R})$. Treating the laser pulses perturbatively, the first order wavefunction due to P is ($\hbar = 1$) $|\Psi_P(s)\rangle = i \int_{-\infty}^{\infty} ds' e^{-iH_0(s-s')} \{\boldsymbol{\mu} \cdot \boldsymbol{\epsilon}_P(s' - t_P)\} |\Psi_0(s')\rangle$, and the second order wavefunction due to both P and P' is $|\Psi_{PP'}(s)\rangle = i \int_{-\infty}^{\infty} ds' e^{-iH_0(s-s')} \{\boldsymbol{\mu} \cdot \boldsymbol{\epsilon}_{P'}(s')\} |\Psi_P(s')\rangle$. It can be shown that $S_{SE}(T) = \langle \Psi_{PP'}(s) | g \rangle \langle g | \Psi_{PP'}(s) \rangle$ (SI-I [21] and [6, 23]).

Preliminary example.— We will develop some intuition through an illustration, in which we focus on $S_{SE}(T)$. Consider the case where the surfaces of

the singly-excited diabatic states have the same shape, $V_{10}(\mathbf{R}) = V_{01}(\mathbf{R}) + c$, for some constant c (but in general $V_g(\mathbf{R}), V_f(\mathbf{R}) \neq V_e(\mathbf{R}) + c$ for $e = 01, 10$). It is convenient to introduce the excitonic basis $\{|g\rangle, |\alpha\rangle, |\beta\rangle, |f\rangle\}$, which diagonalizes the electronic Hamiltonian at the ground state nuclear configuration: $H_{el}(\mathbf{0}) = \omega_g|g\rangle\langle g| + \omega_\alpha|\alpha\rangle\langle\alpha| + \omega_\beta|\beta\rangle\langle\beta| + \omega_f|f\rangle\langle f|$. Here, $|g\rangle = |00\rangle$ and $|f\rangle = |11\rangle$, but in general, $|\alpha\rangle$ and $|\beta\rangle$ differ from $|01\rangle$ and $|10\rangle$ in that they are delocalized due to $J(\mathbf{0})$. Note that both $|\alpha\rangle$ and $|\beta\rangle$ are coupled in the same way to the vibrational bath, and hence they form a decoherence-free subspace [25]. The first order wavefunction “right before” the probe pulse may be expanded as $|\Psi_P(t_1 + T)\rangle = \sum_{i=\alpha,\beta} \sum_m c_{i,m}(T) |i\rangle |\nu_m^{(i)}\rangle$. Since in this case, $|i\rangle |\nu_m^{(i)}\rangle$ are eigenstates of the molecular Hamiltonian $H_0(\mathbf{R})$, the excitons are the adiabatic electronic states, there is no dissipation in the electronic system, and the values $|c_{i,m}(T)|^2$ are constants as a function of T , depending only on the details of P [28]. The wavefunction “right after” the probe at time T is, in the Condon approximation, given by, $|\Psi_{PP'}(t_1 + T)\rangle = i \sum_{i=\alpha,\beta} \sum_{mn} \boldsymbol{\mu}_{mg} \cdot \mathbf{e}_{P'} \tilde{\epsilon}_{P'}(\omega_{im,gn}) \langle \nu_n^{(g)} | \nu_m^{(i)} \rangle c_{i,m}(T) |g\rangle |\nu_n^{(g)}\rangle$, where $\tilde{\epsilon}_p(\omega) = \lambda e^{-(\omega - \omega_p)^2 \sigma^2 / 2}$ is the Fourier transform of pulse p at frequency ω . This expression can be interpreted as a wavepacket in the ground state created when the probe couples the vibrational levels of the singly-excited states to the vibrational levels of the ground state via the electric dipole moment, where the amplitudes in the various vibrational levels depends on the probe’s electric field at the given transition energy and the Condon overlap. Computing the norm of the resulting wavepacket,

$$S_{SE}(T) = \sum_{ij=\alpha,\beta} (\boldsymbol{\mu}_{ig} \cdot \mathbf{e}_{P'}) (\boldsymbol{\mu}_{jg} \cdot \mathbf{e}_{P'}) \times \sum_{mm'n} \langle \nu_m^{(j)} | \nu_n^{(g)} \rangle \langle \nu_n^{(g)} | \nu_m^{(i)} \rangle \times \tilde{\epsilon}_{P'}(\omega_{im,gn}) \tilde{\epsilon}_{P'}^*(\omega_{jm',gn}) c_{i,m}(T) c_{j,m'}^*(T) \quad (1)$$

which corresponds to sums of interferences between vibrational states of the same and different excitonic states, respectively, projecting onto the same vibrational state in the ground state. Note that $S_{SE}(T)$ can be written as a linear combination of elements of the full vibronic density matrix $\rho(T) = |\Psi_P(t_1 + T)\rangle \langle \Psi_P(t_1 + T)|$. The terms $\langle i, m | \rho(T) | j, m' \rangle = c_{im}(T) c_{jm'}^*(T)$ for $(i, m) \neq (j, m')$ correspond to *vibronic coherences* and oscillate at the difference frequency between the $|i\rangle|m\rangle$ and the $|j\rangle|m'\rangle$ states. When we consider the broadband (*bb*) limit of Eq. (1), where $\tilde{\epsilon}(\omega) = \lambda$ for all the ω values of interest,

$$S_{SE}^{bb}(T) = \lambda^2 \sum_{ij=\alpha,\beta} (\boldsymbol{\mu}_{ig} \cdot \mathbf{e}_{P'}) (\boldsymbol{\mu}_{jg} \cdot \mathbf{e}_{P'}) \sum_m c_{im}(T) c_{jm}^*(T) \quad (2)$$

Crucially, Eq. (2) is a linear combination of elements of $\rho_{el}(T)$ as opposed to the full vibronic space. In fact,

the terms for $i = j$ correspond to electronic populations and, due to the absence of electronic decoherence in this example, stay constant with respect to T . The term $\langle \alpha | \rho_{el}(T) | \beta \rangle = \sum_i c_{i,\alpha}(T) c_{i,\beta}^*(T)$ corresponds to an electronic coherence between $|\alpha\rangle$ and $|\beta\rangle$, and shows oscillations at the single frequency $\omega_{\alpha\beta}$ as a function of T . Hence, coherent oscillations in $S_{SE}^{bb}(T)$ are a witness for coherent electronic dynamics. Remarkably, in the additional limit where one of the excitons is dark (e.g., $\boldsymbol{\mu}_{\beta g} = 0$), we have a monomer instead of a dimer, and $S_{SE}^{bb}(T)$ is a constant even in the case of large Condon displacements, where there is large vibrational motion between pump and probe. This observation for the monomer has been previously reported by Yan and Mukamel [26].

The results above can be interpreted as follows. In the Condon approximation, the probe couples only to the electronic dipole, so in the broadband limit it acts uniformly across every transition energy, and hence across every nuclear configuration within a particular electronic state. In general, $S_{SE}(T)$ is a sum of multiple interferences among portions of wavepackets at different electronic and nuclear configurations. In $S_{SE}^{bb}(T)$, the probe opens only two interference pathways (just as in the double-slit experiment), via emission from the $|\alpha\rangle$ or the $|\beta\rangle$ state, insensitive to vibrational dynamics, providing a witness for coherent electronic oscillations.

General case.— The example above readily generalizes to include effects of initial thermalized states of the bath, ESA and GSB contributions, and non-adiabatic effects. In the limit of broadband P (SI-II and III, [21]) and P' , each of the contributions to $S_{PP'}^{bb}(T)$ are (SI-II, [21]), $S_{SE}^{bb}(T) = \lambda^4 \sum_{ijpq} (\boldsymbol{\mu}_{gi} \cdot \mathbf{e}_{P'}) (\boldsymbol{\mu}_{qg} \cdot \mathbf{e}_P) (\boldsymbol{\mu}_{gp} \cdot \mathbf{e}_P) (\boldsymbol{\mu}_{jg} \cdot \mathbf{e}_{P'}) \chi_{ijqp}(T)$, $S_{ESA}^{bb}(T) = -\lambda^4 \sum_{ijpq} (\boldsymbol{\mu}_{fi} \cdot \mathbf{e}_{P'}) (\boldsymbol{\mu}_{qg} \cdot \mathbf{e}_P) (\boldsymbol{\mu}_{gp} \cdot \mathbf{e}_P) (\boldsymbol{\mu}_{jf} \cdot \mathbf{e}_{P'}) \chi_{ijqp}(T)$, and $S_{GSB}^{bb}(T) = \lambda^4 \sum_{ip} (\boldsymbol{\mu}_{gp} \cdot \mathbf{e}_P) (\boldsymbol{\mu}_{pg} \cdot \mathbf{e}_P) (\boldsymbol{\mu}_{gi} \cdot \mathbf{e}_{P'}) (\boldsymbol{\mu}_{ig} \cdot \mathbf{e}_{P'})$, where the *process matrix* $\chi(T)$ is given by, $\chi_{ijqp}(T) = \text{Tr}_{nuc} \{ |i\rangle \langle i| e^{-iH_0 T} (|q\rangle \langle p| \otimes \rho_B(0)) e^{iH_0 T} |j\rangle \}$ [17, 18], and it is easy to see that $S_{PP'}^{bb}(T)$ is invariant under change of electronic basis within the singly-excited states. Here, $\rho_B(0) = \sum_n p_n |\nu_n^{(g)}\rangle \langle \nu_n^{(g)}|$ is the initial thermal vibrational ensemble in the ground electronic state. $\chi(T)$ describes the evolution of the electronic system, assuming that the vibrational system begins in $\rho_B(0)$. If the initial state of the bath can be prepared at $\rho_B(0)$ regardless of the electronic state, as in the impulsive limit, an integrated equation of motion can be written as $\rho_{ij}(T) = \sum_{ijqp} \chi_{ijqp}(T) \rho_{qp}(0)$. As in the preliminary example, $S_{PP'}^{bb}(T)$ is a linear combination of entries of reduced states $\rho_{el}(T)$, so oscillations in it are a manifestation of electronic oscillations, justifying the witness.

Given an electronic basis, any element $\chi_{ijqp}(T)$ can in principle exhibit oscillations. For a large variety of systems, it is however, possible to associate the largest amplitude oscillations of $\chi(T)$ to electronic coherences

in some basis. In the preliminary example, the lack of dissipation implies that $\chi_{ijqp}(T) = \delta_{iq}\delta_{jp}e^{-i\omega_{qp}T}$, so the only possible oscillatory contribution to $S_{PP'}(T)$ corresponds to $\chi_{\alpha\beta\alpha\beta}(T) = \chi_{\beta\alpha\beta\alpha}^*(T)$ (excitonic coherence). In the non-adiabatic case where $V_{01}(\mathbf{R}) \neq V_{10}(\mathbf{R}) + c$, each electronic state couples differently to the vibrational modes. However, in the limit of weak system-bath coupling, the vibronic states $|e\rangle|\nu_j^{(e)}\rangle$ are still the correct eigenstates of $H_0(\mathbf{R})$ up to zeroth order in the coupling, so any oscillations in the signal will still be dominated by excitonic coherences. Finally, for intermediate and strong system-bath coupling together with a fast bath decorrelation timescale, a polaron transformation defines an electronic basis $\{|g\rangle, |\tilde{\alpha}\rangle, |\tilde{\beta}\rangle, |f\rangle\}$ that diagonalizes a zeroth-order electronic Hamiltonian weakly coupled to a renormalized bath ([12] and SI-IV [21]). In this case, the highest amplitude oscillations in its $S_{PP'}^{bb}(T)$ would correspond to electronic coherences $\chi_{\tilde{\alpha}\tilde{\beta}\tilde{\alpha}\tilde{\beta}}(T) = \chi_{\tilde{\beta}\tilde{\alpha}\tilde{\beta}\tilde{\alpha}}^*(T)$. For more general aggregates, if this were an issue of interest, a partial QPT could be designed to determine the value of specific terms of $\chi(T)$ [17, 18].

Numerical examples.— We have performed simulations for a monomer, a dimer which exhibits coherent electronic oscillations, and an incoherent dimer, where each singly-excited site is coupled to a single vibrational mode. These three examples illustrate the value of the witness (Fig. 1), as all three have oscillatory 2D-ES (Fig. 2), but the monomer and incoherent dimer do not have coherent electronic oscillations. The witness correctly shows that only the coherent dimer has a positive witness. The simulations include inhomogeneous broadening (ensembles of 500 molecules with Gaussian site disorder of standard deviation 40 cm⁻¹ and, for the dimers, site energy correlation 0.8), thermal averaging of initial vibrational states according to a Boltzmann distribution at 273 K, isotropic averaging, and explicit inclusion of pulses with the dynamics. Roughly, there are two energy scales to consider, an average coupling J and a reorganization energy λ , in which case the impulsive limit is set by $\frac{1}{\sigma} \gg \max(J, \lambda)$. For these simulations, the pulses are within the FWHM=10–20 fs range, and cover the entire absorption spectra, respectively (SI-V, [21]). Fig. 1 shows $\langle S_{PP'}^{bb}(T) \rangle_{zzzz}$, the witness averaged at the collinear pulse setting $zzzz$, for about 900 fs (top). We can associate the witness oscillations to oscillations of elements in $\chi(T)$. We show a few representative elements of this matrix (bottom). Fig. 2 presents snapshots of the rephasing 2D-ES, $\langle \tilde{S}(\omega_\tau, T, \omega_t) \rangle_{zzzz}$, for a sampling of waiting times T between 71.6 and 270.6 fs (left), indicating that vibronic coherences manifest as diagonal and cross-peak oscillations [29]. Notice that due to strong coupling to vibrations, the coherent dimer also exhibits oscillations in the diagonal peaks, implying the inapplicability of previous measures for this case [13, 14]. As another illustration, the integrated signal under the cross-peaks encircled in

black is in the right plots. Note that the largest amplitude oscillations are in the monomer, which cannot have coherent electronic oscillations, showing that oscillations in peaks in the 2D-ES do not directly translate into coherent electronic dynamics, and hence are not the correct witness.

The witness is positive if, once the dc background is subtracted from $S_{PP'}^{bb}(T)$, there are oscillations with amplitude proportional to μ^4 , where μ is some estimate of an *electronic* transition dipole moment. If spurious oscillations due to finite pulse-duration are suspected, a more quantitative confirmation is the following: (a) Collect traces $S_{PP'}^{bb}(T)$ at several pulse widths σ , all roughly in the broadband domain. (b) Fourier transform the data: $\tilde{S}_{PP'}^{bb}(\omega_T) = \frac{1}{2\pi} \int_0^\infty dT e^{i\omega T} S_{PP'}^{bb}(T)$. (c) Locate non-zero frequencies of $\tilde{S}_{PP'}^{bb}(\omega_T)$ corresponding to oscillations between discrete states (ignore the dc component). For each of these frequencies ω_T , plot $\tilde{S}_{PP'}^{bb}(\omega_T)$ as a function of σ , and linearly extrapolate to $\sigma \rightarrow 0$. If the obtained intercepts are at zero within noise levels, the witness is negative. SI-II [21] displays an analytical expression for the $O(\sigma)$ correction of $S_{PP'}^{bb}(T)$, providing a theoretical basis for this procedure.

Although the theory has been detailed here for a dimer, the witness is applicable to larger aggregates. In the case of FMO, due to spectral congestion, it might be fruitful to focus on pairs of exciton states at a time, for instance, the first and the third exciton states, either via direct PP' measurements that cover these transitions exclusively, or alternatively, integrating windows of broadband 2D-ES corresponding to these two states only, assuming that relaxation processes do not occur outside of this spectral window.

We dedicate this letter to the late Bob Silbey who at different stages introduced J.Y.Z. to theoretical chemistry and mentored A.A.G in the field. We thank DARPA Award No. N66001-10-4060 and EFRC-DOE Award No. de-sc0001088.

* Electronic address: aspuru@chemistry.harvard.edu

- [1] M. Mohseni, P. Rebentrost, S. Lloyd, and A. Aspuru-Guzik, Environment-assisted quantum walks in photosynthetic energy transfer. *J. Chem. Phys.*, 129:174106, 2008.
- [2] M. B. Plenio and S. F. Huelga, *New J. Phys.*, 10:113019, 2008.
- [3] G. S. Engel, T. R. Calhoun, E. L. Read, T. K. Ahn, T. Mancal, Y. C. Cheng, R. E. Blankenship, and G. R. Fleming, *Nature*, 446:782–786, 2007.
- [4] E. Collini, C. Y. Wong, K. E. Wilk, P. M. G. Curmi, P. Brumer, and G. D. Scholes, *Nature*, 463:644–U69, 2010.
- [5] G. Panitchayangkoon, D. Hayes, K. A. Fransted, J. R. Caram, E. Harel, J. Wen, R. E. Blankenship, and G. S. Engel, *Proc. Natl. Acad. Sci. USA*, 107(29):12766–12770,

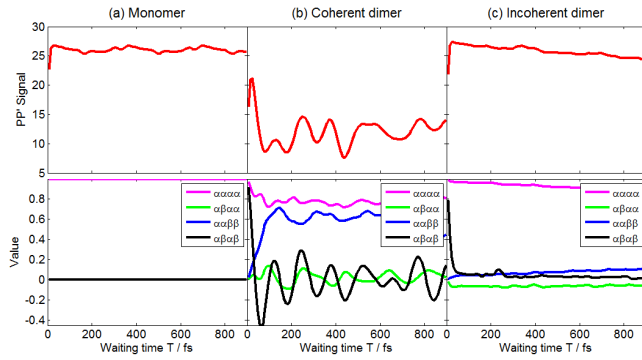


Figure 1: (Top) Broadband PP' spectra as a function of waiting time T as a witness for coherent electronic oscillations. The small oscillations in (a) and (c) are due to finite pulse durations. (Bottom) The witness is a linear combination of elements of the process matrix $\chi(T)$. Traces of a few representative elements of $\chi(T)$ are displayed.

- 2010.
- [6] D. Egorova, *Chem. Phys.*, 347(1-3):166 – 176, 2008.
 - [7] N. Christensson, F. Milota, J. Hauer, J. Sperling, O. Bixner, A. Nemeth, and H. F. Kauffmann, *J. Phys. Chem. B*, 115(18):5383–5391, 2011.
 - [8] N. Christensson, H. F. Kauffmann, T. Pullerits, and T. Mancal, *arXiv:1201.6325 [quant-ph]*.
 - [9] J. D. Biggs and J. A. Cina, *J. Phys. Chem. A*, 116(7):1683–1693, 2012.
 - [10] A. W. Chin, J. Prior, R. Rosenbach, F. Caycedo-Soler, S. F. Huelga, and M. B. Plenio, *arXiv:1203.0776 [quant-ph]*.
 - [11] J. M. Womick and A. M. Moran, *J. Phys. Chem. B*, 115(6):1347–1356, 2011.
 - [12] S. Shim, P. Rebentrost, S. Valleau, and A. Aspuru-Guzik, *Biophys. J.*, 102(3):649 – 660, 2012.
 - [13] Y. C. Cheng and G. R. Fleming, *J. Phys. Chem. A*, 112:4254–4260, 2008.
 - [14] D. B. Turner, K. E. Wilk, P. M. G. Curmi, and G. D. Scholes, *J. Phys. Chem. Lett.*, 2(15):1904–1911, 2011.
 - [15] G. Panitchayangkoon, D. V. Voronine, D. Abramavicius, J. R. Caram, N. H. C. Lewis, S. Mukamel, and G. S. Engel, *Proc. Nat. Acad. Sci. USA*, 108(52):20908–20912, 2011.
 - [16] J. D. Biggs and J. A. Cina, *J. Chem. Phys.*, 131:224101, 2009.
 - [17] J. Yuen-Zhou and A. Aspuru-Guzik, *J. Chem. Phys.*, 134(13):134505, 2011.
 - [18] J. Yuen-Zhou, J. J. Krich, M. Mohseni, and A. Aspuru-Guzik, *Proc. Nat. Acad. Sci. USA*, 108(43):17615, 2011.
 - [19] T. Forster, in *Modern Quantum Chemistry*, volume 3, pages 93–137, Academic Press Inc., New York, 1965.
 - [20] S. Mukamel, *Principles of Nonlinear Optical Spectroscopy*, Oxford University Press, 1995.
 - [21] Supplemental material for this article.
 - [22] M. Cho, *Two Dimensional Optical Spectroscopy*, CRC Press, 2009.
 - [23] D. J. Tannor, *Introduction to Quantum Mechanics: A Time Dependent Approach*, University Science Books, 2007.
 - [24] J. A. Cina and G. R. Fleming, *J. Phys. Chem. A*, 108(51):11196–11208, 2004.

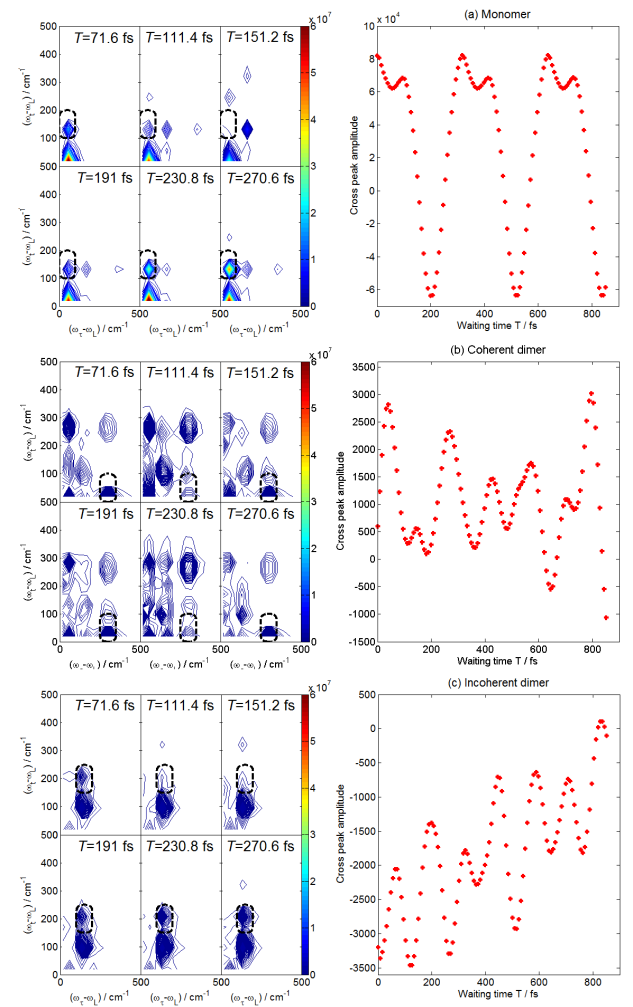


Figure 2: (Left) Norm of broadband rephasing 2D-ES for (a) monomer, (b) coherent dimer, and (c) incoherent dimer. Diagonal and cross peaks oscillate as a function of time in all cases, indicating general vibronic coherences but not necessarily electronic coherence. Color scale (arbitrary units) is fixed throughout. Black dotted circles at left indicate cross peaks whose real part amplitude is shown followed in a finer time grid in the right panels (varying axes for each sample, arbitrary units). These traces are the wrong witness for coherent electronic oscillations.

- [25] D. A. Lidar, I. L. Chuang, and K. B. Whaley, *Phys. Rev. Lett.*, 81:2594–2597, Sep 1998.
- [26] Y. J. Yan and S. Mukamel, *Phys. Rev. A*, 41:6485–6504, Jun 1990.
- [27] R. Silbey and R. A. Harris, *J. Chem. Phys.*, 80(6):2615–2617, 1984.
- [28] This is within the assumptions of the model; e.g., T must be shorter than the fluorescence timescale, $T < 1$ ns, approximately.
- [29] Inhomogeneous broadening was not included in the 2D-ES due to the expensive cost of their computation.

Supplementary Information

PP' SIGNAL IN TERMS OF WAVEPACKET OVERLAPS

Consider the situation described in the article, where the total Hamiltonian is given by $H = H_0(\mathbf{R}) + H_{\text{pert}}(s)$. In this section, we will assume $H_0(\mathbf{R})$ to be the same molecular piece as the one described in the article, and $H_{\text{pert}}(s) = -\boldsymbol{\mu} \cdot \boldsymbol{\epsilon}(\mathbf{r}, s)$ to be the standard light-matter interaction in the dipole approximation, although we consider a slightly more general setup, where the electric field is described by three non-collinear beams, $\boldsymbol{\epsilon}(\mathbf{r}, s) = \sum_{p=1}^3 [\epsilon_p(s - t_p) e^{i\mathbf{k}_p \cdot \mathbf{r} + i\phi_p} \mathbf{e}_p + \text{c.c.}]$ with different wavevectors \mathbf{k}_p and phases ϕ_p . The expressions for $S_{PP'}(T)$ will appear as we take the limit of the PE signal to the PP' limit.

The pulses generate a time-dependent polarization $\mathbf{P}(\mathbf{r}, s) = \text{Tr}(\boldsymbol{\mu}\rho(\mathbf{r})) = \sum_{\mathbf{k}} P(\mathbf{k}; s) e^{i\mathbf{k} \cdot \mathbf{r}}$ on each molecule at position \mathbf{r} [19]. The allowed wavevectors are the phase-matching directions $\mathbf{k} = q\mathbf{k}_1 + r\mathbf{k}_2 + s\mathbf{k}_3$ for integers q, r, s , and encode different sequences of interactions of the pulses with the molecule. We are interested in the signal S at the photon-echo (PE) phase-matched direction $\mathbf{k}_{PE} = -\mathbf{k}_1 + \mathbf{k}_2 + \mathbf{k}_3$, which can be detected by mixing the material ensemble emission with a local oscillator (LO) pulse $\epsilon_4(s)$ travelling along $\mathbf{k}_4 = \mathbf{k}_{PE}$, $S(\tau, T, t) = -2\Im \int_{-\infty}^{\infty} ds \epsilon_4^*(s - t_4) \mathbf{e}_4 \cdot \mathbf{P}(\mathbf{k}_{PE}; \tau, T, s)$, where $\tau = t_2 - t_1$ (coherence time), $T = t_3 - t_2$ (waiting time), and $t = t_4 - t_3$ (echo time) [1]. Upon repeated collection of $S(\tau, T, t)$ for many values of time intervals, a 2D-ES can be constructed as a function of T , by Fourier transforming the signal with respect to τ and t , $\tilde{S}(\omega_\tau, T, \omega_t) = \int_0^\infty d\tau e^{-i\omega_\tau \tau} \int_0^\infty dt e^{i\omega_t t} S(\tau, T, t)$ [2, 3]. In general, oscillations in $S(\tau, T, t)$ and $\tilde{S}(\omega_\tau, T, \omega_t)$ can be associated to coherent superpositions of vibronic eigenstates of $H_0(\mathbf{R})$, but not necessarily of electronic states [4]. In the article, we paid special attention to the pump-probe (PP) limit $S_{PP'}(T)$, which is equivalent to a *differential transmission* signal, where the first two pulses act as the pump P, ($\epsilon_1 = \epsilon_2 \equiv \epsilon_P$, $\phi_1 = \phi_2 \equiv \phi_P$), the last two as the probe P' ($\epsilon_3 = \epsilon_4 \equiv \epsilon_{P'}$ and $\phi_3 = \phi_4 \equiv \phi_{P'}$), $\tau = t = 0$, and P and P' are well separated (i.e., $T \gg \sigma$). $S_{PP'}(T)$ can be recovered from the 2D-ES as an inverse Fourier transform at zero frequencies, $S_{PP'}(T) \equiv S_{PE}(0, T, 0) = \frac{1}{(2\pi)^2} \int_{-\infty}^{\infty} d\omega_\tau \int_{-\infty}^{\infty} d\omega_t \tilde{S}(\omega_\tau, T, \omega_t)$. This limit justifies the form of $H_{\text{pert}}(s)$ given in the article, which only consists of two pulses.

The starting point is the expression for $S_{PP'}(T)$,

$$S_{PP'}(T) = -2\Im \int_{-\infty}^{\infty} ds' \epsilon_4^*(s' - t_4) \mathbf{e}_4 \cdot \mathbf{P}(\mathbf{k}_{PE}; 0, T, 0). \quad (\text{S1})$$

We shall derive a wavepacket overlap formula for $S_{PP'}(T)$ assuming that P and P' are well separated, $T \gg \sigma$, analogously to the doorway-window approach [1]. First, we conveniently define the following wavefunctions:

$$|\Psi_0(s)\rangle = e^{-iH_0(s-t_P)} |\Psi_0(s')\rangle, \quad (\text{S2})$$

$$|\Psi_P(s)\rangle = i \int_{-\infty}^{\infty} ds' e^{-iH_0(s-s')} \{\boldsymbol{\mu} \cdot \mathbf{e}_P(\epsilon_P(s' - t_P) + \text{c.c.})\} |\Psi_0(s')\rangle, \quad (\text{S3})$$

$$|\Psi_{P'}(s)\rangle = i \int_{-\infty}^{\infty} ds' e^{-iH_0(s-s')} \{\boldsymbol{\mu} \cdot \mathbf{e}_{P'}(\epsilon_{P'}(s' - t_{P'}) + \text{c.c.})\} |\Psi_{P'}(s')\rangle, \quad (\text{S4})$$

$$\begin{aligned} |\Psi_{PP}(s)\rangle &= (i)^2 \int_{-\infty}^{\infty} ds' \int_{-\infty}^{s'} ds'' e^{-iH_0(s-s')} \{\boldsymbol{\mu} \cdot \mathbf{e}_P(\epsilon_P(s' - t_P) + \text{c.c.})\} \\ &\quad \times e^{-iH_0(s'-s'')} \{\boldsymbol{\mu} \cdot \mathbf{e}_P(\epsilon_P(s'' - t_P) + \text{c.c.})\} |\Psi_0(s'')\rangle, \end{aligned} \quad (\text{S5})$$

$$\begin{aligned} |\Psi_{P'P'}(s)\rangle &= (i)^2 \int_{-\infty}^{\infty} ds' \int_{-\infty}^{s'} ds'' e^{-iH_0(s-s')} \{\boldsymbol{\mu} \cdot \mathbf{e}_{P'}(\epsilon_{P'}(s' - t_{P'}) + \text{c.c.})\} \\ &\quad \times e^{-iH_0(s'-s'')} \{\boldsymbol{\mu} \cdot \mathbf{e}_{P'}(\epsilon_{P'}(s'' - t_{P'}) + \text{c.c.})\} |\Psi_0(s'')\rangle, \end{aligned} \quad (\text{S6})$$

$$\begin{aligned} |\Psi_{PP'P'}(s)\rangle &= (i)^2 \int_{-\infty}^{\infty} ds' \int_{-\infty}^{s'} ds'' e^{-iH_0(s-s')} \{\boldsymbol{\mu} \cdot \mathbf{e}_{P'}(\epsilon_{P'}(s' - t_{P'}) + \text{c.c.})\} \\ &\quad \times e^{-iH_0(s'-s'')} \{\boldsymbol{\mu} \cdot \mathbf{e}_{P'}(\epsilon_{P'}(s'' - t_{P'}) + \text{c.c.})\} |\Psi_{PP}(s'')\rangle, \end{aligned} \quad (\text{S7})$$

which are valid for $s \gg t_{P'}$ (after the envelopes of the pulses have considerably decayed), and which correspond to the processes indicated by their subscripts, i.e., $|\Psi_{PP'P'}(s)\rangle$ corresponds to the fourth order wavefunction ($O(\lambda^4)$) resulting from two actions of P and two of P' (see Fig. S1).

Eqs. (S2)–(S7) allow for a calculation of $\mathbf{P}(\mathbf{k}_{PE}; 0, T, 0)$ and hence of $S_{PP'}(T)$ via Eq. (S1). Note that, as opposed to a general PE signal, $S_{PP'}(T)$ does not depend on the phases of the pulses because $\phi_1 = \phi_2 \equiv \phi_P$ and $\phi_3 = \phi_4 \equiv \phi_{P'}$. The phase-matching condition $\mathbf{k}_{PE} = -\mathbf{k}_1 + \mathbf{k}_2 + \mathbf{k}_3$ together with the rotating-wave approximation indicate that for each wavevector $+\mathbf{k}_j(-\mathbf{k}_j)$, the pulse j acts with the term $\epsilon_j(\epsilon_j^*)$, exciting (de-exciting) the ket or de-exciting (exciting) the bra. Collecting all the terms result in $S_{PP'}(T) = S_{SE}(T) + S_{ESA}(T) + S_{GSB}(T)$:

$$\begin{aligned} S_{SE}(T) &= -2\Im \int_{-\infty}^{\infty} dt' \langle \Psi_{PP'}(t') | \{ \epsilon_{P'}^*(t' - t_{P'}) \boldsymbol{\mu} \cdot \mathbf{e}_{P'} \} | \Psi_P(t') \rangle \\ &= -2\Im(-i) \int_{-\infty}^{\infty} dt' \int_{-\infty}^{t'} ds' \langle \Psi_P(s') | \{ -i\epsilon_{P'}(s' - t_{P'}) \boldsymbol{\mu} \cdot \mathbf{e}_{P'} \} e^{iH_0(t' - s')} \{ (i)\epsilon_{P'}^*(t' - t_{P'}) \boldsymbol{\mu} \cdot \mathbf{e}_{P'} \} | \Psi_P(t') \rangle \\ &= 2\langle \Psi_{PP'}(s) | g \rangle \langle g | \Psi_{PP'}(s) \rangle, \end{aligned} \quad (S8)$$

$$\begin{aligned} S_{ESA}(T) &= -2\Im \int_{-\infty}^{\infty} dt' \langle \Psi_P(t') | \{ \epsilon_{P'}^*(t' - t_{P'}) \boldsymbol{\mu} \cdot \mathbf{e}_{P'} \} | \Psi_{PP'}(t') \rangle \\ &= -2\Im(i) \int_{-\infty}^{\infty} dt' \int_{-\infty}^{t'} ds' \langle \Psi_P(t') | \{ (-i)\epsilon_{P'}^*(t' - t_{P'}) \boldsymbol{\mu} \cdot \mathbf{e}_P \} e^{-iH_0(t' - s')} \{ i\epsilon_P(s' - t_P) \boldsymbol{\mu} \cdot \mathbf{e}_P \} | \Psi_P(s') \rangle \\ &= -2\langle \Psi_{PP'}(s) | f \rangle \langle f | \Psi_{PP'}(s) \rangle, \end{aligned} \quad (S9)$$

$$\begin{aligned} S_{GSB}(T) &= -2\Im \int_{-\infty}^{\infty} dt' \{ \langle \Psi_{PP}(t') | \{ \epsilon_{P'}^*(t' - t_{P'}) \boldsymbol{\mu} \cdot \mathbf{e}_{P'} \} | \Psi_{P'}(t') \rangle + \langle \Psi_0(t') | \{ \epsilon_{P'}^*(t' - t_{P'}) \boldsymbol{\mu} \cdot \mathbf{e}_{P'} \} | \Psi_{PP'P'}(t') \rangle \} \\ &= -2\Im(-i) \int_{-\infty}^{\infty} dt' \{ \langle \Psi_{PP}(t') | \{ (i)\epsilon_{P'}^*(t' - t_{P'}) \boldsymbol{\mu} \cdot \mathbf{e}_{P'} \} | \Psi_{P'}(t') \rangle + \langle \Psi_0(t') | \{ (i)\epsilon_{P'}^*(t' - t_{P'}) \boldsymbol{\mu} \cdot \mathbf{e}_{P'} \} | \Psi_{PP'P'}(t') \rangle \} \\ &= 2\Re \{ \langle \Psi_{PP}(s) | g \rangle \langle g | \Psi_{P'P'}(s) \rangle + \langle \Psi_0(s) | g \rangle \langle g | \Psi_{PP'P'}(s) \rangle \}. \end{aligned} \quad (S10)$$

where again, $s \gg t_{P'}$, and otherwise, the signals are independent of s . This can be easily understood in physical terms: After the action of the pulses, the wavefunctions still evolve according to $H_0(\mathbf{R})$, but the overlaps do not change in time. Eqs. (S8)–(S10) are in the spirit of wavepacket approaches to PP' spectroscopy [5–11].

In order to gain additional insight, we interpret the formulas in terms of differential transmission by enumerating all the possible absorption and emission processes which are quadratic in P and P'. P promotes a wavepacket from $|g\rangle$ to $|\Psi_P(s)\rangle$, a superposition of wavepackets in $|\alpha\rangle$ and $|\beta\rangle$. P' acts on this state, creating $|\Psi_{PP'}(s)\rangle$, a superposition of wavepackets in $|g\rangle$ and $|f\rangle$. Naturally, the photons emitted in SE correspond to the squared amplitude of $\langle g | \Psi_{PP'}(t) \rangle$, whereas the ones absorbed in ESA are associated with the squared amplitude of $\langle f | \Psi_{PP'}(s) \rangle$, hence providing an intuition for the expressions for $S_{SE}(T)$ and $S_{ESA}(T)$. Finally, $S_{GSB}(T)$ can be thought as accounting for the “leftover” SE processes, namely, overlaps between wavepackets created by pulses at different times. After P and P', the total ground state wavepacket is $\langle g | \Psi(t) \rangle = \langle g | (|\Psi_0(t)\rangle + |\Psi_{PP'}(t)\rangle + |\Psi_{PP}(t)\rangle + |\Psi_{P'P'}(t)\rangle + |\Psi_{PP'P'}(t)\rangle + \text{higher order contributions})$. Collecting wavepacket overlaps which are quadratic in both pulses yields $S_{SE}(T) + S_{GSB}(T)$. “Leftover” ESA processes do not contribute to $S_{PP'}(T)$ because they do not fulfill the PE phase-matching condition (they appear in double-quantum coherence spectroscopy, for instance).

Thermal effects follow from averaging the signals corresponding to initial states $|\Psi_0(t_P)\rangle$ sampled according to a Boltzmann distribution.

GENERAL EXPRESSIONS FOR $S_{PP'}(T)$ IN VIBRONIC BASIS

In order to manipulate the wavepacket overlap expressions, it is convenient to define two vibronic bases:

- The vibronic eigenbasis of $H_0(\mathbf{R})$, $\{|g, \nu_n^{(g)}\rangle, |\zeta\rangle, |f, \nu_n^{(f)}\rangle\}$, which satisfy

$$H_0(\mathbf{R})|g, \nu_n^{(g)}\rangle = \omega_{gn}|\zeta\rangle, \quad (S11)$$

$$H_0(\mathbf{R})|\zeta\rangle = \omega_{\zeta}|\zeta\rangle, \quad (S12)$$

$$H_0(\mathbf{R})|f, \nu_n^{(f)}\rangle = \omega_{fn}|f, \nu_n^{(f)}\rangle. \quad (S13)$$

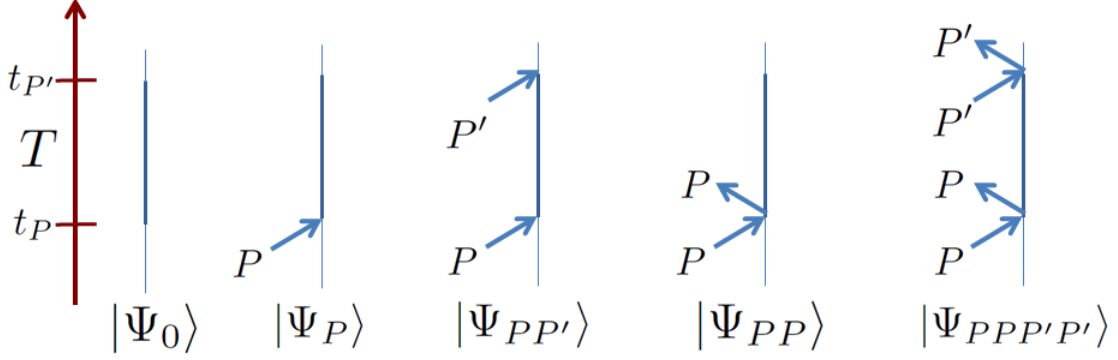


Figure S1: Feynman diagrams for the wavefunctions defined in Eqs. (S2)–(S7).

where $|\zeta\rangle$ corresponds to the singly excited state manifold.

- The tensor product basis $\{|m, \nu_n^{(g)}\rangle\}$, where $\{|m\rangle\}$ denotes electronic states in an arbitrary electronic basis (for instance, the excitonic one), and $\{|\nu_n^{(g)}\rangle\}$ refers to vibrational eigenstates of the ground vibrational Hamiltonian, $H_{vib,00}(\mathbf{R}) = T_N + V_{00}(\mathbf{R})$.

Note that we can always write states in the vibronic eigenbasis in terms of the second one: $|g, \nu_n^{(g)}\rangle$ stays the same, $|\zeta\rangle = \sum_{mn} \langle m, \nu_n^{(g)} | \zeta \rangle |m, \nu_n^{(g)}\rangle$, and $|f, \nu_{n'}^{(f)}\rangle = \sum_n |f, \nu_{n'}^{(g)}\rangle \langle f, \nu_n^{(g)} | f, \nu_{n'}^{(f)} \rangle = \sum_n \langle \nu_n^{(g)} | \nu_{n'}^{(f)} \rangle |f, \nu_n^{(g)}\rangle$.

Using both bases, the process matrix $\chi(T)$ affords a compact representation,

$$\begin{aligned} \chi_{ijqp}(T) &= \chi_{ijqp}(T) = \text{Tr}_{nuc} \{ \langle i | e^{-iH_0 T} (|q\rangle \langle p| \otimes \rho_B(0)) e^{iH_0 T} | j \rangle \} \\ &= \sum_{\zeta \zeta' n n'} p_n e^{-i(\omega_\zeta - \omega_{\zeta'}) T} \langle i, \nu_{n'}^{(g)} | \zeta \rangle \langle \zeta | q, \nu_n^{(g)} \rangle \langle p, \nu_n^{(g)} | \zeta' \rangle \langle \zeta' | j, \nu_{n'}^{(g)} \rangle. \end{aligned} \quad (\text{S14})$$

Our goal is to write $S_{PP'}(T)$ for arbitrary bandwidth in a similar style, so that in the broadband limit, we can identify it as a linear combinations of elements of $\chi(T)$, hence proving Eqs. (S22)–(S24) in the article. We start by rewriting Eqs. (S2)–(S7) in the vibronic bases:

$$\begin{aligned} |\Psi_{PP'}(s)\rangle &= - \sum_{iq} (\boldsymbol{\mu}_{gi} \cdot \mathbf{e}_{P'}) (\boldsymbol{\mu}_{qg} \cdot \mathbf{e}_P) \sum_{\zeta n'} \langle i, \nu_{n'}^{(g)} | \zeta \rangle \langle \zeta | q, \nu_n^{(g)} \rangle e^{-i\omega_\zeta (s-t_1)} \\ &\quad \times \left(\sum_m \langle \nu_m^{(f)} | \nu_{n'}^{(g)} \rangle \tilde{\epsilon}_{P'}(\omega_{fm, \zeta}) \tilde{\epsilon}_P(\omega_{\zeta, gn}) |f\rangle + \tilde{\epsilon}_{P'}(\omega_{\zeta, gn'}) \tilde{\epsilon}_P(\omega_{\zeta, gn}) |g\rangle \right) |\nu_{n'}^{(g)}\rangle, \end{aligned} \quad (\text{S15})$$

$$\begin{aligned} |\Psi_{PP}(s)\rangle &= - \sum_{iq} (\boldsymbol{\mu}_{ig} \cdot \mathbf{e}_P) (\boldsymbol{\mu}_{qg} \cdot \mathbf{e}_P) \sum_{\zeta n'} \langle i, \nu_{n'}^{(g)} | \zeta \rangle \langle \zeta | q, \nu_n^{(g)} \rangle e^{-i\omega_{gn'} (s-t_1)} \\ &\quad \times \frac{1}{2} \tilde{\epsilon}_P(\omega_{gn', \zeta}) \tilde{\epsilon}_P(\omega_{\zeta, gn}) \left(1 - \text{Erf} \left(\frac{i\sigma((\omega_L + \omega_{gn', \zeta}) + (\omega_L - \omega_{\zeta, gn}))}{2} \right) \right) |g\rangle |\nu_{n'}^{(g)}\rangle, \end{aligned} \quad (\text{S16})$$

$$\begin{aligned} |\Psi_{P'P'}(s)\rangle &= - \sum_{jp} (\boldsymbol{\mu}_{ig} \cdot \mathbf{e}_{P'}) (\boldsymbol{\mu}_{pg} \cdot \mathbf{e}_{P'}) \sum_{\zeta n'} \langle j, \nu_{n'}^{(g)} | \zeta \rangle \langle \zeta | p, \nu_n^{(g)} \rangle e^{-i\omega_{gn'} (s-t_2)} \\ &\quad \times \frac{1}{2} \tilde{\epsilon}_P(\omega_{gn', \zeta}) \tilde{\epsilon}_P(\omega_{\zeta, gn}) \left(1 - \text{Erf} \left(\frac{i\sigma((\omega_L + \omega_{gn', \zeta}) + (\omega_L - \omega_{\zeta, gn}))}{2} \right) \right) |g\rangle |\nu_{n'}^{(g)}\rangle, \end{aligned} \quad (\text{S17})$$

$$\begin{aligned} |\Psi_{PPPP'}(s)\rangle &= \sum_{ijqp} (\boldsymbol{\mu}_{gj} \cdot \mathbf{e}_P) (\boldsymbol{\mu}_{pg} \cdot \mathbf{e}_P) (\boldsymbol{\mu}_{gi} \cdot \mathbf{e}_{P'}) (\boldsymbol{\mu}_{qg} \cdot \mathbf{e}_P) \\ &\quad \times \sum_{\zeta' \zeta n n' n''} \langle j, \nu_{n'}^{(g)} | \zeta' \rangle \langle \zeta' | p, \nu_{n'}^{(g)} \rangle \langle i, \nu_{n'}^{(g)} | \zeta \rangle \langle \zeta | q, \nu_n^{(g)} \rangle e^{-i\omega_{gn'} (s-t_1)} \\ &\quad \times \frac{1}{4} \tilde{\epsilon}_{P'}(\omega_{gn'', \zeta'}) \tilde{\epsilon}_{P'}(\omega_{\zeta', gn'}) \tilde{\epsilon}_P(\omega_{gn', \zeta}) \tilde{\epsilon}_P(\omega_{\zeta, gn}) \end{aligned}$$

$$\begin{aligned}
& \times \left(1 - \text{Erf} \left(\frac{i\sigma((\omega_L + \omega_{gn''}, \zeta) + (\omega_L - \omega_{\zeta', gn'}))}{2} \right) \right) \\
& \times \left(1 - \text{Erf} \left(\frac{i\sigma((\omega_L + \omega_{gn', \zeta}) + (\omega_L - \omega_{\zeta, gn}))}{2} \right) \right) |g\rangle |\nu_{n''}^{(g)}\rangle.
\end{aligned} \tag{S18}$$

where the Erf functions appear due to pulse overlap. Eqs. (S8)–(S10) together with Eqs. (S15)–(S18) yield:

$$\begin{aligned}
S_{SE}(T) &= \sum_{ijqp} (\boldsymbol{\mu}_{gi} \cdot \mathbf{e}_{P'}) (\boldsymbol{\mu}_{qg} \cdot \mathbf{e}_P) (\boldsymbol{\mu}_{gp} \cdot \mathbf{e}_P) (\boldsymbol{\mu}_{jg} \cdot \mathbf{e}_{P'}) \sum_{\zeta \zeta' nn'} \tilde{\epsilon}_{P'}(\omega_{gn'}, \zeta) \tilde{\epsilon}_P(\omega_{\zeta, gn}) \tilde{\epsilon}_P(\omega_{gn, \zeta'}) \tilde{\epsilon}_{P'}(\omega_{\zeta', gn'}) \\
&\quad \times p_n e^{-i(\omega_{\zeta} - \omega_{\zeta'})T} \langle i, \nu_{n'}^{(g)} | \zeta \rangle \langle \zeta | q, \nu_n^{(g)} \rangle \langle p, \nu_n^{(g)} | \zeta' \rangle \langle \zeta' | j, \nu_{n''}^{(g)} \rangle,
\end{aligned} \tag{S19}$$

$$\begin{aligned}
S_{ESA}(T) &= - \sum_{ijqp} (\boldsymbol{\mu}_{fi} \cdot \mathbf{e}_{P'}) (\boldsymbol{\mu}_{qg} \cdot \mathbf{e}_P) (\boldsymbol{\mu}_{gp} \cdot \mathbf{e}_P) (\boldsymbol{\mu}_{jf} \cdot \mathbf{e}_{P'}) \\
&\quad \times \sum_{\zeta \zeta' nn' n'' m} \langle \nu_{n''}^{(g)} | \nu_m^{(f)} \rangle \langle \nu_m^{(f)} | \nu_{n'}^{(g)} \rangle \tilde{\epsilon}_{P'}(\omega_{fm, \zeta}) \tilde{\epsilon}_P(\omega_{\zeta, gn}) \tilde{\epsilon}_P(\omega_{gn, \zeta'}) \tilde{\epsilon}_{P'}(\omega_{\zeta', fm}) \\
&\quad \times p_n e^{-i(\omega_{\zeta} - \omega_{\zeta'})T} \langle i, \nu_{n'}^{(g)} | \zeta \rangle \langle \zeta | q, \nu_n^{(g)} \rangle \langle p, \nu_n^{(g)} | \zeta' \rangle \langle \zeta' | j, \nu_{n''}^{(g)} \rangle,
\end{aligned} \tag{S20}$$

$$\begin{aligned}
S_{GSB}(T) &= 2\Re \sum_{ijqp} (\boldsymbol{\mu}_{gi} \cdot \mathbf{e}_{P'}) (\boldsymbol{\mu}_{qg} \cdot \mathbf{e}_{P'}) (\boldsymbol{\mu}_{gp} \cdot \mathbf{e}_P) (\boldsymbol{\mu}_{jg} \cdot \mathbf{e}_P) \left(\frac{1}{4} \right) \sum_{\zeta \zeta' nn'} \tilde{\epsilon}_{P'}(\omega_{gn'}, \zeta) \tilde{\epsilon}_{P'}(\omega_{\zeta, gn}) \tilde{\epsilon}_P(\omega_{gn, \zeta'}) \tilde{\epsilon}_P(\omega_{\zeta', gn'}) \\
&\quad \times \left\{ p_n \langle i, \nu_{n'}^{(g)} | \zeta \rangle \langle \zeta | q, \nu_n^{(g)} \rangle \langle p, \nu_n^{(g)} | \zeta' \rangle \langle \zeta' | j, \nu_{n''}^{(g)} \rangle e^{-i\omega_{gn, gn'} T} \right. \\
&\quad \times \left(1 - \text{Erf} \left(\frac{i\sigma((-\omega_{gn'}, \zeta - \omega_L) + (\omega_{\zeta, gn} - \omega_L))}{2} \right) \right) \left(1 - \text{Erf} \left(\frac{i\sigma((-\omega_{gn, \zeta'} - \omega_L) + (\omega_{\zeta', gn'} - \omega_L))}{2} \right) \right)^* \\
&\quad + p_n \langle i, \nu_{n'}^{(g)} | \zeta \rangle \langle \zeta | q, \nu_n^{(g)} \rangle \left(\langle p, \nu_n^{(g)} | \zeta' \rangle \langle \zeta' | j, \nu_{n''}^{(g)} \rangle e^{i\omega_{gn', gn} T} \right)^* \\
&\quad \times \left(1 - \text{Erf} \left(\frac{i\sigma((-\omega_{gn'}, \zeta - \omega_L) + (\omega_{\zeta, gn} - \omega_L))}{2} \right) \right) \left(1 - \text{Erf} \left(\frac{i\sigma((-\omega_{gn, \zeta'} - \omega_L) + (\omega_{\zeta', gn'} - \omega_L))}{2} \right) \right)^* \Big\}
\end{aligned}$$

The expressions above can be intuitively understood in terms of the double-sided Feynman diagrams in Fig. S2. The expression for GSB consists of a sum of terms corresponding to two types of Feynman pathways which are different in general.

In the broadband limit where $\tilde{\epsilon}_P(\omega) = \tilde{\epsilon}_{P'}(\omega) = \lambda$, many sums above collapse through resolutions of the identity, and we straightforwardly recover the expressions in the article,

$$S_{SE}^{bb}(T) = \lambda^4 \sum_{ijpq} (\boldsymbol{\mu}_{gi} \cdot \mathbf{e}_{P'}) (\boldsymbol{\mu}_{qg} \cdot \mathbf{e}_P) \tag{S22}$$

$$\begin{aligned}
& \times (\boldsymbol{\mu}_{gp} \cdot \mathbf{e}_P) (\boldsymbol{\mu}_{jg} \cdot \mathbf{e}_{P'}) \chi_{ijqp}(T), \\
S_{ESA}^{bb}(T) &= -\lambda^4 \sum_{ijpq} (\boldsymbol{\mu}_{fi} \cdot \mathbf{e}_{P'}) (\boldsymbol{\mu}_{qg} \cdot \mathbf{e}_P) \tag{S23}
\end{aligned}$$

$$\begin{aligned}
& \times (\boldsymbol{\mu}_{gp} \cdot \mathbf{e}_P) (\boldsymbol{\mu}_{jf} \cdot \mathbf{e}_{P'}) \chi_{ijqp}(T), \\
S_{GSB}^{bb}(T) &= \lambda^4 \sum_{ip} (\boldsymbol{\mu}_{gp} \cdot \mathbf{e}_P) (\boldsymbol{\mu}_{pg} \cdot \mathbf{e}_P) \tag{S24} \\
& \times (\boldsymbol{\mu}_{gi} \cdot \mathbf{e}_{P'}) (\boldsymbol{\mu}_{ig} \cdot \mathbf{e}_{P'}).
\end{aligned}$$

In this limit, as highlighted by the T -independent form of Eq. (S24), the two types of GSB pathways yield the same stationary background to the signal (caused by copies of the initial stationary wavepackets in the ground electronic surface).

In the practical case where the pulses are broad, but not infinitely sharp in time, we can expand, $S_{PP'}(T) = S_{PP'}^{bb}(T) + S_{PP'}^{(1)}(T)$ where $S_{PP'}^{(1)}(T) = S_{GSB}^{(1)}(T)$ corresponds to corrections of $O(\sigma)$, which originate from the Erf functions in the GSB signal:

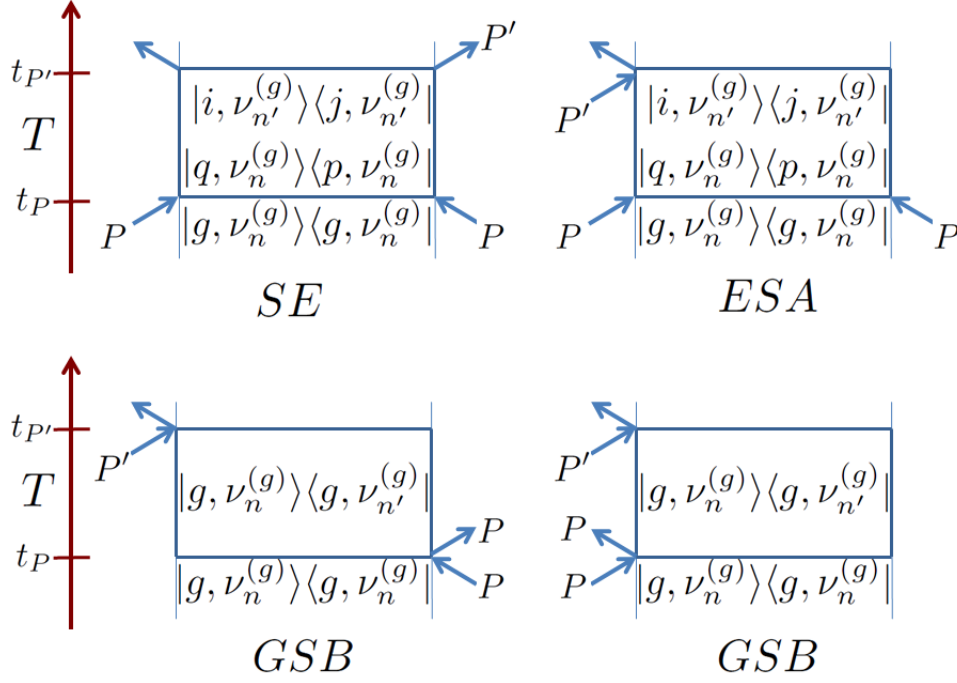


Figure S2: Double-sided Feynman diagrams for general PP' signal.

$$\begin{aligned}
S_{GSB}^{(1)}(T) = & -\frac{\lambda^4}{2} \sum_{ijqp} (\boldsymbol{\mu}_{gi} \cdot \mathbf{e}_{P'}) (\boldsymbol{\mu}_{qg} \cdot \mathbf{e}_{P'}) (\boldsymbol{\mu}_{gp} \cdot \mathbf{e}_P) (\boldsymbol{\mu}_{jg} \cdot \mathbf{e}_P) \\
& \times \Re \left\{ \sum_{\zeta \zeta' nn'} p_n \langle i, \nu_n^{(g)} | \zeta \rangle \langle \zeta | q, \nu_n^{(g)} \rangle \langle p, \nu_n^{(g)} | \zeta' \rangle \langle \zeta' | j, \nu_n^{(g)} \rangle e^{-i\omega_{gn,gn'} T} \right. \\
& \times \frac{i((- \omega_{gn',\zeta} - \omega_L) + (\omega_{\zeta,gn} - \omega_L))}{\sqrt{\pi}} + \frac{-i((- \omega_{gn,\zeta'} - \omega_L) + (\omega_{\zeta',gn'} - \omega_L))}{\sqrt{\pi}} \\
& + \sum_{\zeta \zeta' nn'} p_n \langle i, \nu_n^{(g)} | \zeta \rangle \langle \zeta | q, \nu_n^{(g)} \rangle \left(\langle p, \nu_n^{(g)} | \zeta' \rangle \langle \zeta' | j, \nu_n^{(g)} \rangle e^{i\omega_{gn',gn} T} \right)^* \\
& \left. + \frac{i((- \omega_{gn',\zeta} - \omega_L) + (\omega_{\zeta,gn} - \omega_L))}{\sqrt{\pi}} + \frac{i((- \omega_{gn,\zeta'} - \omega_L) + (\omega_{\zeta',gn'} - \omega_L))}{\sqrt{\pi}} \right\} \sigma.
\end{aligned}$$

SE and ESA processes only contribute to corrections of $O(\sigma^2)$ via the Gaussian spectral profile of the pulses.

REQUIREMENT OF BROADBAND PUMP P

Although the conclusions of the preliminary example in the article hold even in the case of narrowband P', we also require broad bandwidth for P for two reasons:

1. *Non-stationary GSB contributions.* Eqs. (S5) and (S7) show that in the limit of broadband P, this pulse promotes a wavepacket to the excited states and immediately back down to $|g\rangle$, yielding a wavefunction $|\Psi_{PP}(t)\rangle$ that is proportional to the original $|\Psi_0(t_P)\rangle$ before any pulse (also see Eq. S24). In this limit, as emphasized in the previous section, $S_{GSB}(T)$ is a constant background as a function of T , giving the opportunity to identify $S_{PP'}(T)$ as a probe for singly-excited state dynamics. Under a narrowband P, this no longer holds, as shown by Eq. (S21), which depends on T in general. In this case, $|\Psi_{PP}(t)\rangle$ will be a non-stationary wavepacket in the ground electronic surface, which will manifest as time-evolving overlaps both in $\langle \Psi_{PP}(s) | g \rangle \langle g | \Psi_{P'P'}(s) \rangle$ and in $\langle \Psi_0(s) | g \rangle \langle g | \Psi_{PP'P'}(s) \rangle$ (see Eq. (S10)).

2. *Consistency with QPT.* As mentioned in the article, the initial states prepared under a broadband P are of the form $\rho(0) = |q\rangle\langle p| \otimes \rho_B(0)$, where $\rho_B(0) = \sum_n p_n |\nu_n^{(g)}\rangle\langle \nu_n^{(g)}|$ is the initial thermal ensemble of vibrations in the ground electronic surface for all $|q\rangle\langle p|$. Under a narrowband P, it is not possible to prepare initial tensor product states between the system and a fixed bath ρ_B , so $S_{PP'}(T)$ can no longer be written in terms of elements of a single $\chi(T)$, and the equation $\rho(T) = \chi(T)\rho(0)$ loses its meaning.

POLARON TRANSFORMATION

Here, we summarize the essential features of the polaron transformation used in the arguments of the article. We closely follow the works of Silbey, Harris, and coworkers [12–14]. Consider the approximation where the diabatic potential energy surfaces are given by harmonic wells along each nuclear coordinate, $V_{10}(\mathbf{R}) = E_{10} + \sum_n \frac{m_n \omega_n^2 R_n^2}{2} + \sqrt{2m_n \omega_n^3} g_{10,n} R_n$, and $V_{01}(\mathbf{R})$ has the same form except for the substitution $10 \rightarrow 01$ in the subscripts, whereas $V_g(\mathbf{R})$ and $V_f(\mathbf{R})$ have arbitrary shapes. Here, ω_n denotes the n -th mode frequency, whereas the displacements $g_{10,n}$ denote linear couplings of the electronic system to the nuclear bath. Define the harmonic oscillator creation and annihilation operators in the usual way $b_n^\dagger = \sqrt{\frac{m_n}{2}} x_n \mp \frac{1}{\sqrt{2m_n \omega_n}} \frac{\partial}{\partial x_n}$, and also the generator $G = \sum_n (b_n^\dagger - b_n)(g_{10,n}|10\rangle\langle 10| + g_{01,n}|01\rangle\langle 01|)$ such that $U = e^G$ corresponds to a unitary transformation of the full-polaron transformation [14]. It follows that $\tilde{H}(\mathbf{R}) \equiv e^G H_0(\mathbf{R}) e^{-G} = \tilde{H}_0(\mathbf{R}) + \tilde{H}_1(\mathbf{R})$, where $\tilde{H}_0(\mathbf{R}) = T_N + \tilde{H}_{el}(\mathbf{R})$ is our new zeroth-order Hamiltonian, and $\tilde{H}_1(\mathbf{R})$ is the perturbation term, whenever it is small compared to $\tilde{H}_0(\mathbf{R})$. To make a connection with the previous notation, we explicitly write $\tilde{H}_{el} = \sum_{mn} \tilde{V}_{mn} |mn\rangle\langle mn| + \tilde{J}(|10\rangle\langle 01| + |01\rangle\langle 10|)$, where,

$$\begin{aligned} \tilde{V}_{10} &= E_{10} - \sum_n \omega_n g_{10,n}^2 + \sum_n \frac{m_n \omega_n^2 R_n^2}{2}, \\ \tilde{V}_{01} &= E_{01} - \sum_n \omega_n g_{01,n}^2 + \sum_n \frac{m_n \omega_n^2 R_n^2}{2}, \\ \tilde{J} &= J\langle w \rangle, \\ w &= \exp \left(\sum_n (g_{10,n} - g_{01,n})(b_n^\dagger - b_n) \right), \\ \langle w \rangle &= \text{Tr}(w \rho_B(0)) \\ &= \exp \left(- \sum_n \coth \frac{\beta \omega_n (g_{nD} - g_{nA})^2}{2} \right). \end{aligned}$$

The expressions β , $\rho_B(0) = \prod_n \sum_r \frac{\exp(-\beta \omega_n (r + \frac{1}{2})) |\omega_n, r\rangle\langle \omega_n, r|}{Z_n(\beta)}$, $Z_n(\beta) = \frac{1}{2 \sinh(\beta \omega_n / 2)}$, $|\omega_n, r\rangle$ label the inverse temperature, the initial thermal ensemble of vibrations, the partition function of the n -th oscillator, and the r -th eigenstate of the n -th harmonic oscillator, respectively. \tilde{J} can be interpreted as a renormalized site-site coupling due to phonon-dressing. Furthermore, $\tilde{H}_1(\mathbf{R}) = J(w - \langle w \rangle)|10\rangle\langle 01| + \text{h.c.}$ Jang advises to consider the smallness of the quantity $J\sqrt{1 - w^2}$ as the figure of merit for the validity of perturbation theory, and hence for the usefulness of the polaron transformation. Cao and coworkers note that the accuracy of the polaron transformation is guaranteed only in the scenario of fast bath decorrelation compared to the other relevant timescales [15].

If the dynamics of all the degrees of freedom are governed by $\tilde{H}_0(\mathbf{R})$ alone, the electronic system is effectively uncoupled from the nuclear bath. The diagonalization of $\tilde{H}_0(0)$ yields polaronic states $\{|g\rangle, |\tilde{\alpha}\rangle, |\tilde{\beta}\rangle, |f\rangle\}$ which satisfy $\chi_{ijqp}(T) = \delta_{iq} \delta_{jp} e^{-i\omega_{qp}T}$. As can be easily checked, Eqs. (S22–S24) are invariant under change of basis. Hence, if $\tilde{H}_1(\mathbf{R})$ can be guaranteed to be a small perturbation for $\tilde{H}_0(\mathbf{R})$, to zeroth-order in $\tilde{H}_1(\mathbf{R})$, the coherent electronic oscillations in $S_{PP'}^{bb}(T)$ correspond to electronic coherences in the polaronic basis.

The steps above have been outlined for the full-polaron transformation, but the conclusion can be easily seen to hold whenever the total Hamiltonian can be repartitioned into a large contribution and a small system-bath coupling. Examples include the variational polaron transformation [12, 13], which interpolates between weak and strong coupling between the original system and bath, as well transformations which include anharmonicities in the diabatic potential energy surfaces (quadratic coupling between the original system and bath, [16]).

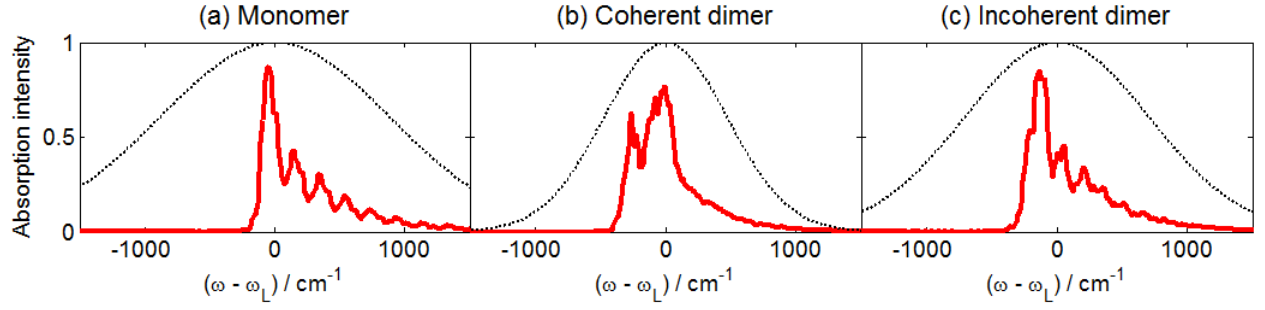


Figure S3: Inhomogeneously broadened absorption spectra (solid red) with pulse spectral profiles $|\tilde{\epsilon}_p(\omega)|^2$ on top (dotted black).

DETAILS OF THE NUMERICAL SIMULATIONS IN THE ARTICLE

We have performed computational simulations [20] for absorption spectra, PP' signal, and rephasing 2D-ES for a monomer, a dimer which exhibits electronic coherent oscillations, and an incoherent dimer. For their Hamiltonians, we choose harmonic diabatic surfaces parametrized by $V_{mn}(x, y) = E_{mn} + \frac{\omega_{mn,x}^2(x - \Delta_{mn,x})^2}{2} + \frac{\omega_{mn,y}^2(y - \Delta_{mn,y})^2}{2}$, where x and y are scaled nuclear coordinates, E_{mn} are site energies, $\omega_{mn,x(y)}$ are oscillator frequencies and $\Delta_{mn,x(y)}$ are electron-nuclear couplings [6–8, 17, 18]. The parameters for the calculations are listed in Table 1. We assumed that $V_f(x, y) = V_{10}(x, y) + V_{01}(x, y)$, and that the carrier frequency of all the pulses is $\omega_p = \omega_L$. The dimers are such that the dipoles are oriented 90 degrees from each other, and the ratio between their norms is 1:3.

Fig. S1 shows inhomogeneously and rotationally averaged absorption spectra (solid red) for the examples used in the numerical simulations of the article. The pulse profiles (dotted black lines) which roughly cover the strongest vibronic transitions with similar amplitude, giving a qualitative idea of what broadband means in practice. In these examples, $\text{FWHM} = 2\sqrt{2\ln 2}\sigma = 10, 18.7$, and 12.5 fs, for the monomer, coherent dimer, and incoherent dimer cases, respectively.

TABLE 1. Parameters of simulations

	M	CD	ID
E_{00}/cm^{-1}	0	0	0
$\langle E_{10} - \omega_L \rangle / \text{cm}^{-1}$	-125	-300	-200
$\langle E_{01} - \omega_L \rangle / \text{cm}^{-1}$	—	-200	-200
J/cm^{-1}	—	100	10
$\omega_{00,x} = \omega_{00,y}/\text{cm}^{-1}$	100	100	100
$\omega_{10,x} = \omega_{01,x}/\text{cm}^{-1}$	200	200	200
$\omega_{10,y} = \omega_{01,y}/\text{cm}^{-1}$	150	150	150
$\Delta_{00,x}/\text{cm}^{1/2}$	0	0	0
$\Delta_{00,y}/\text{cm}^{1/2}$	0	0	0
$\Delta_{10,x}/\text{cm}^{1/2}$	100	50	100
$\Delta_{10,y}/\text{cm}^{1/2}$	0	0	0
$\Delta_{01,x}/\text{cm}^{1/2}$	0	0	0
$\Delta_{01,y}/\text{cm}^{1/2}$	100	50	100
$\text{FWHM} = 2\sqrt{2\ln 2}\sigma/\text{fs}$	10	18.7	12.5

* Electronic address: aspu@chemistry.harvard.edu

- [1] S. Mukamel, *Principles of Nonlinear Optical Spectroscopy*, Oxford University Press, 1995.
- [2] S. Mukamel, *Ann. Rev. Phys. Chem.*, 51(1):691–729, 2000.
- [3] M. Cho, *Two Dimensional Optical Spectroscopy*, CRC Press, 2009.
- [4] D. Egorova, *Chem. Phys.*, 347(1-3):166 – 176, 2008.
- [5] S. Mukamel, C. Ciordas-Ciurdariu, and V. Khidekel, *Advances in Chemical Physics*, pages 345–372. John Wiley and Sons, Inc., 2007.

- [6] J. A. Cina and G. R. Fleming, *J. Phys. Chem. A*, 108(51):11196–11208, 2004.
- [7] J. D. Biggs and J. A. Cina, *J. Chem. Phys.*, 131:224101, 2009.
- [8] J. D. Biggs and J. A. Cina, *J. Chem. Phys.*, 131:224302, 2009.
- [9] J. D. Biggs and J. A. Cina, *J. Phys. Chem. A*, 116(7):1683–1693, 2012.
- [10] Jianshu Cao and Kent R. Wilson, *J. Chem. Phys.*, 106(12):5062–5072, 1997.
- [11] S.Y. Lee, in *Femtosecond Chemistry*, pages 273–298. Wiley-VCH Verlag GmbH, 2008.
- [12] R. Silbey and R. A. Harris, *J. Chem. Phys.*, 80(6):2615–2617, 1984.
- [13] R. A. Harris and R. Silbey, *J. Chem. Phys.*, 83(3):1069–1074, 1985.
- [14] S. Jang, *J. Chem. Phys.*, 131(16):164101, 2009.
- [15] C. Kong Lee, J. Moix, and J. Cao, *arXiv:1201.2436 [quant-ph]*.
- [16] R. W. Munn and R. Silbey, *J. Chem. Phys.*, 68(5):2439–2450, 1978.
- [17] T. Forster, in *Modern Quantum Chemistry*, volume 3, pages 93–137, Academic Press Inc., New York, 1965.
- [18] J. A. Cina, D. S. Kilin, and T. S. Humble, *J. Chem. Phys.*, 118:46–61, 2003.
- [19] We use the word *polarization* in two different ways: To denote (a) the orientation of oscillations of the electric field and (b) the density of electric dipole moments in a material. The meaning should be clear by the context.
- [20] Details of the computational methodology will be presented elsewhere.